

Current in nanojunctions : Effects of reservoir coupling

Hari Kumar Yadalam, Upendra Harbola

Department of Inorganic and Physical Chemistry, Indian Institute of Science, Bangalore 560012, India.

Abstract

We study the effect of system reservoir coupling on currents flowing through quantum junctions. We consider two simple double-quantum dot configurations coupled to two external fermionic reservoirs and study the net current flowing between the two reservoirs. The net current is partitioned into currents carried by the eigenstates of the system and by the coherences between the eigenstates induced due to coupling with the reservoirs. We find that current carried by populations is always positive whereas current carried by coherences are negative for large couplings. This results in a non-monotonic dependence of the net current on the coupling strength. We find that in certain cases, the net current can vanish at large couplings due to cancellation between currents carried by the eigenstates and by the coherences. These results provide new insights into the non-trivial role of system-reservoir couplings on electron transport through quantum dot junctions. In the presence of weak coulomb interactions, net current as a function of system reservoir coupling strength shows similar trends as for the non-interacting case.

Keywords: Nanojunctions, Electron transport, System-reservoir coupling strength

1. Introduction

Transport properties of quantum junctions have been studied for over two decades motivated not only by their technological relevance but also the opportunities they provide to explore fundamental physics. For example quantum dot junctions provide a good platform for verification of fundamental concepts, like fluctuation theorems [1, 2]. There have also been a lot of technologically relevant proposals of diodes [3], transistors [4], heat engines [5, 6], which can be realized using quantum junctions made of single molecules or quantum dots. Quantum dot junctions can also serve as promising candidates for realizing quantum computers [7].

Current flowing through quantum dot junctions [8] and molecular junctions [9, 10, 11, 12, 13] have been measured experimentally and studied using various theoretical formulations like quantum master equations (QME) [14], scattering matrix (SM) [15], and non equilibrium Green's function (NEGF) method [16]. QME and SM approaches are valid within a certain parameter regime, but NEGF method is exact and can be applied in all regimes, although analytically tractable results can be obtained only for non-interacting systems.

Although a good amount of theoretical work on quantum conduction exists in the literature [15], however the role of system-reservoir coupling has not been explored much, except for few works. For example in experiments performed with carbon nanotube junctions reported in Ref.[17], the importance of non-point like contact of reservoir system coupling was observed. The effect of finite contact length was studied in Ref. [18] using tight binding models, and it was demonstrated that the transmission can be enhanced at lower system reservoir coupling strengths by increasing the contact length. Further, in Ref.[19], the effect of reservoir induced coupling between

quantum dots on the current was studied. It is important to note here that, the system-reservoir coupling strength can be tuned using external gate potentials in quantum dot junctions [8] and can be tuned in molecular junctions [20] by tuning the density of states of metal near fermi-energy [21, 22, 23], by tuning orbital overlaps of metal and molecule [24] or by chemical gating [25].

To gain more understanding on the role of system reservoir coupling strength, we ask the question, "How does the current vary as system-reservoir coupling is changed?". To answer this question, we note that, in a simple scattering picture, the system-reservoir coupling offers (contact) resistance to the tunneling electrons. Within the quantum master equation formulation (Lindblad quantum master equation), the current increases monotonically as the coupling is increased. However, this does not present the complete picture and it is not at all obvious what happens as one goes beyond the regime of QME or simple scattering picture. In Ref.[26], scattering formalism under weak reservoir coupling was used to study the effect of reservoir induced coherences on the net current through a coupled double-quantum dot model.

In this work we explore the effect of strong system-reservoir couplings on the net current flowing through quantum junctions using NEGF formulation. The advantages of the NEGF formulation over the other formulations discussed above are two folds. First, in most practical cases, it provides an exact method to compute the current in molecular junctions. Secondly, this is a standard well established method to include effects arising due to many-body interactions, as we shall discuss in the later part of this paper.

In the following, we find that the net current is not always an increasing function of the coupling strength. In fact, sur-

prisingly, we find that for certain cases the net current may diminish at large coupling strengths. As we discuss below, this surprising behavior is a consequence of the quantum interference between the eigenstates which carries a negative (against the applied bias) current that may cancel the currents coming from the eigenstates. In the absence of the interferences, the net current always shows a monotonic increase with the reservoir couplings. The current behavior for large couplings, of course, depends on the quantum dot configuration and is not universal. For certain configurations, there is an optimal value of the coupling strength at which the current is maximal. A similar non-monotonic behavior of heat current in spin-boson model[27, 28] and of energy flux through externally driven molecular junction[29] has been observed.

Recently the effect of quantum interference on current flowing through molecular junctions has been studied experimentally [30, 31, 32, 33] and theoretically [34, 35, 36, 37, 38, 39]. Various device proposals making use of quantum interference effects have been made, see for example quantum transistor [4], thermoelectric engines [40, 41, 42], molecular switch [43]. It was shown both experimentally and theoretically that vibrations suppress destructive interference effect leading to enhancement of current [44, 45]. In a recent work by Markussen and Thygesen [46], the effect of temperature on the junction conductance has been studied using interacting quantum dot model. The interference effect was shown to lead to stronger temperature dependence of conductance. In the present work, however, we focus on interference effects in the strong molecule-reservoir coupling regime where such effects are significant and play a crucial role, as discussed below. We find that the temperature (broadening of fermi functions) only makes small quantitative changes, the qualitative behavior of the junction conductance remains the same.

To explore this current behavior we consider two simple (non-interacting) models both consist of two quantum dots coupled to two fermionic reservoirs but differ in their configurations. This is discussed in the next section.

2. Model Hamiltonian and current calculation

We start by considering a simple model shown in Fig. 1. It consists of two quantum dots each having a single electron orbital coupled to each other and also coupled to two fermionic reservoirs.

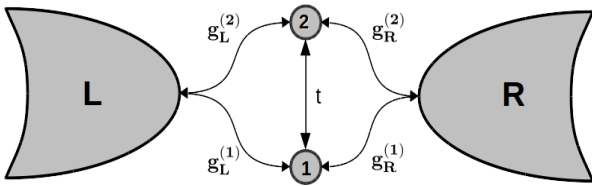


Figure 1: Schematic of the model system considered. It consists of two localized sites coupled to two fermionic reservoirs, left (L) and right (R). $g_\alpha^{(x)}$ is the strength of the coupling between the α^{th} reservoir and the x^{th} site and t is the inter-site coupling strength.

The Hamiltonian describing this model is given as,

$$\begin{aligned} \hat{H} &= \sum_{i,j=1}^2 H_{0ij} c_i^\dagger c_j + \sum_k \epsilon_{\alpha,k} d_{\alpha k}^\dagger d_{\alpha k} \\ &+ \sum_k [g_L^{(1)} d_{Lk}^\dagger c_1 + g_R^{(1)} d_{Rk}^\dagger c_1 + g_L^{(2)} d_{Lk}^\dagger c_2 \\ &+ g_R^{(2)} d_{Rk}^\dagger c_2 + h.c.] \end{aligned} \quad (1)$$

where

$$H_0 = \begin{pmatrix} \epsilon_1 & -t \\ -t & \epsilon_2 \end{pmatrix} \quad (2)$$

is the single particle Hamiltonian for the isolated molecule. Here c_i (c_i^\dagger) are the fermionic annihilation (creation) operators for destroying (creating) electron at site ' i ' and similarly $d_{\alpha k}$ ($d_{\alpha k}^\dagger$) are operators for destroying (creating) electron in state labeled by ' k ' in the ' α ' reservoir ($\alpha = L/R$). First two terms in the Hamiltonian represent isolated system and reservoir Hamiltonians, and the third term represents hybridization between system and reservoirs with $g_\alpha^{(1)}$ and $g_\alpha^{(2)}$ representing coupling of the α th reservoir with dot (1) and dot (2), respectively. We have also assumed wide-band approximation (system-reservoir coupling is independent of ' k ').

The net current I_L flowing into the left reservoir is given by the rate of change of charge on the left reservoir, i.e., $I_L(t) = \frac{d}{dt} \langle -e \sum_k d_{Lk}^\dagger d_{Lk} \rangle$. The net current can be expressed in terms of system greater and lesser Green's functions [47, 16] $G^{>/<}$ as ,

$$I_L = \frac{e}{h} \int_{-\infty}^{+\infty} d\omega \text{Tr} [\Sigma_L^<(\omega) G^>(\omega) - G^<(\omega) \Sigma_L^>(\omega)], \quad (3)$$

where $\Sigma_L^{>/<}(\omega)$ and $G^{>/<}(\omega)$ are (energy domain) Fourier transformed greater and lesser projections of contour-ordered self-energy due to left reservoir and the system Greens' functions [48]. A similar expression, obtained by replacing $L \leftrightarrow R$ in Eq. (3), holds true for the right current, I_R . At steady state the left and the right currents must be the same in magnitude, $|I_R| = |I_L|$, which is referred to as the left-right symmetry at steady state.

The Green's functions obtained by solving equation of motion[48] in energy domain can be used in Eq. (3) to get expression for the net current, I_L [16, 49].

For simplicity we consider two cases : serially coupled dot system (obtained in the limit $g_L^{(2)} = g_R^{(1)} = 0$) and side coupled dot system (obtained in the limit $g_L^{(2)} = g_R^{(2)} = 0$). We further assume that site energies are same as the Fermi energies of the two reservoirs (set to zero).

The net current for serially coupled dot system is obtained as (we use units such that $e = 1$, and $h = 1$)

$$I_L = \int_{-\infty}^{+\infty} d\omega \left[\frac{\Gamma^2 t^2}{(\omega^2 - t^2 - (\frac{\Gamma}{2})^2)^2 + \omega^2 \Gamma^2} \right] [f_L(\omega) - f_R(\omega)]. \quad (4)$$

For the side coupled dot system, the net current is

$$I_L = \int_{-\infty}^{+\infty} d\omega \left[\frac{\Gamma^2 \omega^2}{(\omega^2 - t^2)^2 + \omega^2 \Gamma^2} \right] [f_L(\omega) - f_R(\omega)]. \quad (5)$$

Here $f_\alpha(\omega) = \frac{1}{e^{\beta_\alpha(\omega-\mu_\alpha)}+1}$ is the Fermi function of two reservoirs ($\alpha = 1, 2$), β_α and μ_α are, respectively, the inverse temperature and the chemical potential of α^{th} reservoir. Here we assumed that all the relevant non-zero couplings to the reservoirs are identical, $g_\alpha^{(x)} = g$. The coupling strength $\Gamma = 2\pi\rho|g|^2$, where ρ is the density of states of the reservoirs assumed to be energy independent and identical for both the reservoirs.

Currents in Eq.(7) and Eq.(8) are plotted against Γ in Fig. (2) for $t = 1$, $\mu_L = 1$, $\mu_R = -1$ and $\beta_L^{-1} = \beta_R^{-1} = 0$. Throughout this work, all the energy scales and currents are expressed in units of t and $\frac{e}{h}t$, respectively. It is clear that the net current is not always

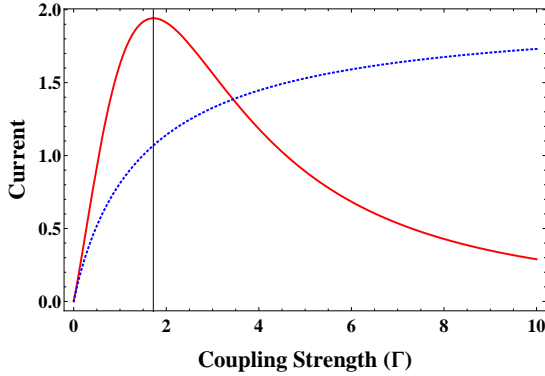


Figure 2: (Color online) Net current as a function of Γ for serially coupled double quantum dot system (red-continuous) and side coupled double quantum dot system (blue-dotted) systems. Here $\beta_L^{-1} = \beta_R^{-1} = 0$, $\mu_L = \frac{V}{2}$ and $\mu_R = -\frac{V}{2}$ with $V = 2$. All energy scales are in units of t and current is in units of et/h with $t = 1$.

an increasing function of Γ . For side coupled dot system, net current is an increasing function of Γ and saturates asymptotically to a constant value for large Γ , which for zero temperature is simply proportional to the difference in chemical potentials of the two reservoirs. However, for serial coupled dot system, the net current shows a non-monotonic behavior and settles to zero for large Γ . The latter case is very counter intuitive and, in order to understand these two completely different current behaviors, below we analyze currents in the eigenbasis of the system.

3. Partitioning the current

We define a unitary transformation matrix, \mathcal{U} , which diagonalizes the system Hamiltonian H_0 , i.e., $\mathcal{U} = \frac{1}{\sqrt{2}} \begin{pmatrix} 1 & 1 \\ 1 & -1 \end{pmatrix}$.

We next transform lesser and greater Green's functions $G^{</>}(\omega)$ and lesser and greater left-reservoir self-energies $\Sigma_L^{</>}(\omega)$ into the eigenbasis using, $A \rightarrow \bar{A} = \mathcal{U}^\dagger A \mathcal{U}$, where A is any matrix defined in the local basis. Thus transforming Eq. (3) to eigenbasis, the net current can be partitioned into currents carried by the population in the bonding state (I_b), population in the anti-bonding state (I_a), and the current carried by coherences between these two states (I_c). The expressions for individual contributions are given as

$$I_b = \int_{-\infty}^{+\infty} d\omega \left[\Sigma_{Lbb}^{<}(\omega) G_{bb}^{>}(\omega) - G_{bb}^{<}(\omega) \Sigma_{Lbb}^{>}(\omega) \right], \quad (6)$$

$$I_a = \int_{-\infty}^{+\infty} d\omega \left[\Sigma_{La a}^{<}(\omega) G_{aa}^{>}(\omega) - G_{aa}^{<}(\omega) \Sigma_{La a}^{>}(\omega) \right] \quad (7)$$

and

$$I_c = \int_{-\infty}^{+\infty} d\omega \left[\Sigma_{Lba}^{<}(\omega) G_{ab}^{>}(\omega) - G_{ab}^{<}(\omega) \Sigma_{Lba}^{>}(\omega) + \Sigma_{Lab}^{<}(\omega) G_{ba}^{>}(\omega) - G_{ba}^{<}(\omega) \Sigma_{Lab}^{>}(\omega) \right]. \quad (8)$$

Partitioning of the net current in Eqs. (6)- (8) is based on the fact that the Greens' functions $G_{xx}^{>}$ and $G_{xx}^{<}$, where $x = a, b$, correspond to the population of state x , while $G_{xy}^{<}$ and $G_{xy}^{>}$ give coherences between the states x and y . Similarly I_R can also be partitioned in terms of currents carried by the populations and the coherences. It is straightforward to show that these currents are individually conserved, i.e, left-right symmetry holds for each current.

We next specialize to two simple models introduced in the previous section to gain a better insight into the role of system reservoir coupling strength on the current.

Serially coupled system : For the serially coupled double quantum dot system, explicit expressions for I_b , I_a and I_c are

$$I_b = \int_{-\infty}^{+\infty} d\omega \left[\frac{(\frac{\Gamma}{2})^2}{(\omega+t)^2 + (\frac{\Gamma}{2})^2} \right] [f_L(\omega) - f_R(\omega)], \quad (9)$$

$$I_a = \int_{-\infty}^{+\infty} d\omega \left[\frac{(\frac{\Gamma}{2})^2}{(\omega-t)^2 + (\frac{\Gamma}{2})^2} \right] [f_L(\omega) - f_R(\omega)] \quad (10)$$

and

$$I_c = \int_{-\infty}^{+\infty} d\omega \left[\frac{-2(\frac{\Gamma}{2})^2 (\omega^2 - t^2 + (\frac{\Gamma}{2})^2)}{(\omega^2 - t^2 - (\frac{\Gamma}{2})^2)^2 + \omega^2 \Gamma^2} \right] [f_L(\omega) - f_R(\omega)]. \quad (11)$$

The above integrals can be easily performed for zero temperature case ($\beta_L^{-1} = \beta_R^{-1} = 0$) to get

$$I_b = \frac{\Gamma}{2} \left[\tan^{-1} \left(\frac{V+2t}{\Gamma} \right) + \tan^{-1} \left(\frac{V-2t}{\Gamma} \right) \right] \quad (12)$$

and $I_a = I_b$ at zero temperature for the symmetrically biased system ($\mu_L = \frac{V}{2}$ and $\mu_R = -\frac{V}{2}$). The coherent contribution is obtained as

$$I_c = \left(\frac{\Gamma^2}{4t^2 + \Gamma^2} \right) \left\{ t \log \left(\frac{(V+2t)^2 + \Gamma^2}{(V-2t)^2 + \Gamma^2} \right) - \Gamma \left[\tan^{-1} \left(\frac{V+2t}{\Gamma} \right) + \tan^{-1} \left(\frac{V-2t}{\Gamma} \right) \right] \right\} \quad (13)$$

The expressions for currents from the bonding and the anti-bonding orbitals, Eqs. (9) and (10), are identical to the one obtained for a single resonant level with energies $-t$ and t , respectively [16]. These contributions are always positive (throughout, we assume $\mu_L > \mu_R$ and the two reservoirs have the same temperature). However, as noted from Eq. (11) or (13), the

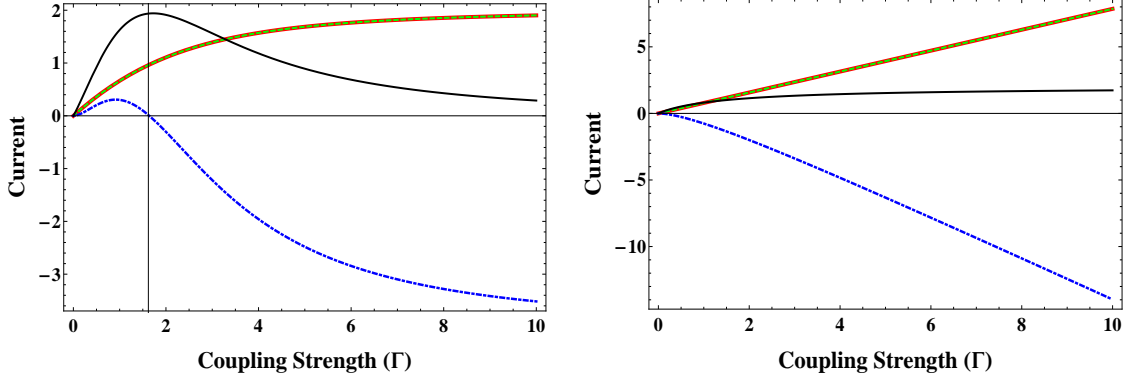


Figure 3: (Color online) Currents carried by population in bonding (red-thick) state, population in anti-bonding (green-dashed) state and coherences between the bonding and anti-bonding states (blue-dot-dashed) along with the net current (black-thin) for serially coupled (left) and side coupled (right) double quantum dot system as a function of Γ with all parameters being same as in Fig. (2).

coherent contribution can be positive or negative depending on the relative values of the coupling strengths Γ and t . For large Γ , the logarithmic term vanishes and coherent contribution is always negative which can compete with the contributions from the populations. Current contributions from eigenstate populations and coherences together with the net current are plotted as a function of Γ in the left panel of Fig. (3). Here bonding and anti-bonding (population) contributions are equal due to the parameters chosen ($\epsilon_1 = \epsilon_2 = 0$ and $\mu_R = -\mu_L$). These contributions increase with Γ and saturate to a non zero constant value for large Γ , which corresponds to unit conductance (e^2/h) per electron channel. The coherent contribution shows non monotonic trend, initially increases but finally settles down to a negative value which is equal to the sum of bonding and anti-bonding contributions for large Γ . This non-monotonic character in I_c is seen only for bias values $V \leq 2t$. For large values of the bias $V \gg 2t$, the coherent contribution is always negative. Thus for intermediate bias values, it should be possible to maximize the net current by suitably choosing the coupling strength. For $V \ll 2t$, the coherent contribution vanishes if $\Gamma = 2t$ and the net current is maximum. For large Γ , the conductivity of the two population channels (bonding and anti-bonding states) is unity (in units of $\frac{e^2}{h}$) while that of the coherent channel approaches to 2, although in the opposite direction to the applied bias. Thus for large Γ , both population channels and coherence channel conduct equal current but in the opposite directions, which leads to a vanishing net current for large Γ .

Side coupled system : Next we consider the case when $g_L^{(2)} = g_R^{(2)} = 0$. In this case the explicit expressions for I_b , I_a and I_c are obtained as follows.

$$I_b = \frac{1}{4} \int_{-\infty}^{+\infty} d\omega \left[\frac{\Gamma^2(\omega - t)^2}{(\omega^2 - t^2)^2 + \omega^2\Gamma^2} \right] [f_L(\omega) - f_R(\omega)], \quad (14)$$

$$I_a = \frac{1}{4} \int_{-\infty}^{+\infty} d\omega \left[\frac{\Gamma^2(\omega + t)^2}{(\omega^2 - t^2)^2 + \omega^2\Gamma^2} \right] [f_L(\omega) - f_R(\omega)] \quad (15)$$

and

$$I_c = \frac{1}{2} \int_{-\infty}^{+\infty} d\omega \left[\frac{\Gamma^2(\omega^2 - t^2)}{(\omega^2 - t^2)^2 + \omega^2\Gamma^2} \right] [f_L(\omega) - f_R(\omega)]. \quad (16)$$

The analytic expressions for these currents for zero temperature case are given by,

$$I_b = \left(\frac{\Gamma}{2}\right)^2 \left\{ \frac{(a_1 - t)^2}{(a_1 - a_2)(a_1 - a_3)(a_1 - a_4)} \log\left(\frac{a_1 - \frac{V}{2}}{a_1 + \frac{V}{2}}\right) + \frac{(a_2 - t)^2}{(a_2 - a_1)(a_2 - a_3)(a_2 - a_4)} \log\left(\frac{a_2 - \frac{V}{2}}{a_2 + \frac{V}{2}}\right) + \frac{(a_3 - t)^2}{(a_3 - a_1)(a_3 - a_2)(a_3 - a_4)} \log\left(\frac{a_3 - \frac{V}{2}}{a_3 + \frac{V}{2}}\right) + \frac{(a_4 - t)^2}{(a_4 - a_1)(a_4 - a_2)(a_4 - a_3)} \log\left(\frac{a_4 - \frac{V}{2}}{a_4 + \frac{V}{2}}\right) \right\}. \quad (17)$$

I_a is obtained by replacing t with $-t$ in Eq. (17), and

$$I_c = \left(\frac{\Gamma}{2}\right)^2 \left\{ \frac{1}{(a_1 - a_2)} \left[\log\left(\frac{a_1 - \frac{V}{2}}{a_1 + \frac{V}{2}}\right) - \log\left(\frac{a_2 - \frac{V}{2}}{a_2 + \frac{V}{2}}\right) \right] + \frac{1}{(a_3 - a_4)} \left[\log\left(\frac{a_3 - \frac{V}{2}}{a_3 + \frac{V}{2}}\right) - \log\left(\frac{a_4 - \frac{V}{2}}{a_4 + \frac{V}{2}}\right) \right] \right\} \quad (18)$$

where $a_1 = -i\frac{\Gamma}{2} + \sqrt{t^2 - (\frac{\Gamma}{2})^2}$, $a_2 = -i\frac{\Gamma}{2} - \sqrt{t^2 - (\frac{\Gamma}{2})^2}$, $a_3 = i\frac{\Gamma}{2} + \sqrt{t^2 - (\frac{\Gamma}{2})^2}$ and $a_4 = i\frac{\Gamma}{2} - \sqrt{t^2 - (\frac{\Gamma}{2})^2}$.

For $\Gamma \gg t$, the current contributions, I_b and I_c , acquire the simple form,

$$I_b = \frac{\Gamma}{2} \left[\tan^{-1}\left(\frac{\Gamma V}{2t^2}\right) + \tan^{-1}\left(\frac{V}{2\Gamma}\right) \right] \\ I_c = \Gamma \left[\tan^{-1}\left(\frac{V}{2\Gamma}\right) - \tan^{-1}\left(\frac{\Gamma V}{2t^2}\right) \right]. \quad (19)$$

Unlike the serially coupled case, in this case both contributions, population as well as the coherences, grow linearly with Γ . However, their sum, the total current, saturates to the value

$\Gamma \tan^{-1}(V/2\Gamma)$. We again notice that contributions from the bonding and the anti-bonding states are always positive while the coherent contribution is always negative for large Γ . This is shown in the right panel of Fig. (3). The rate of increase of the currents through the eigenstates is precisely half of the rate with which current increases (in the opposite direction) via the coherences. Thus the net rate is zero and the total current saturates to a constant value.

In this section, we have derived some analytical results for simple noninteracting model systems to study the effects of system-reservoir coupling on the net current. A natural question arises as to the validity of this result in more realistic systems. To check this, in the following section, we introduce electron-electron interaction in the system. However it becomes difficult to obtain analytic expressions for currents, hence we present results based on numerical calculations.

4. Effect of coulomb interaction

To explore effect of coulomb interaction on the trend observed above, we add the following interaction part to the system Hamiltonian,

$$H_{int} = \frac{1}{2} \sum_{i,j=1,2} V_{ij} c_i^\dagger c_i c_j^\dagger c_j \quad (20)$$

where $V_{ij} = U(1 - \delta_{ij})$. This (Coulomb) interaction leads to an extra self-energy in the equation of motion of the Greens' function[48]. We compute this self-energy within the Hartree-Fock (HF) or mean-field approximation and *GW* approximation[50, 51, 52, 53, 54]. It has been shown in Ref.[55] that within *GW* approximation one can have multiple solutions. However, in the weak interaction limit, $(U/\Gamma) \leq 1$, there is only one unique physical solution.

The equation of motion for the interacting Green's function together with self energies Σ_{ij}^{MF} , Σ_{ij}^{GW} [48] give a set of coupled equations which need to be solved self-consistently. This is done most efficiently in the energy domain. The converged solution of the self-consistent solution for the Greens functions is then used to compute the net current using Eq. (3). We display the net current as a function of coupling strength for various Coulomb interaction strengths calculated within HF approximation in Fig. (4). Inset shows the deviations in the net current calculated within the HF approximation from that calculated within *GW* approximation. As can be seen, the previously observed non-monotonic behavior of the net current for both the serially-coupled as well as the side-coupled cases are robust to weak Coulomb correlations. However, partitioning of the current in terms of the population and coherences, as introduced previously, is more subtle in the presence of interactions.

At the Hartree-Fock level, if the partitioning is done in the single-particle basis renormalized by the mean-field potential, the individual current components satisfy the left-right symmetry as discussed previously. However, if the partitioning is done in the bare single particle basis (rotation by \mathcal{U}), the individual current components do not satisfy the left-right symmetry in case of serially coupled dots. In the side-coupled system, it

turns out, that the left-right symmetry is always satisfied, irrespective of the basis used (rotation by any arbitrary \mathcal{U} matrix). Purely on the physical grounds, we choose to define such a partitioning in the eigenbasis of the renormalized dots where all current components, both in the serially- and the side-coupled cases, satisfy the left-right symmetry. In Fig. (5), we plot these current components as function of the coupling strength. These show qualitatively similar behavior as obtained in the previous section for non-interacting system.

It should be emphasized that within the mean-field approximation, the single-particle picture is still valid and one can write down an effective single-particle Hamiltonian by renormalizing the bare dot energies and couplings. This allows to identify a transformation matrix \mathcal{U} . Such a single-particle description breaks down within the *GW* approximation. Thus identifying the individual current components in the eigenbasis is not possible. In this case, therefore, we analyze the total current which, irrespective of the basis used, always satisfies the left-right symmetry. We find that even within the *GW* approximation, the net current shows similar qualitative behavior with increasing coupling strength as discussed previously. This result is presented in Fig. (4) with a comparison between the HF and the *GW* results.

5. Conclusion

In this work we have explored the effects of system-reservoir coupling on currents through molecular (quantum dot) junctions. It is shown that the net current in a molecular junction is not always a monotonically increasing function of the coupling strength. We have demonstrated this by considering two simple model junctions which are easily realizable in experiments. For a serially arranged double quantum dot system, the net current behaves non-monotonically and goes to zero for large Γ , while for a side-coupled quantum dot system, the current increases monotonically and saturates to a finite non-zero value. These two different current behaviors originate due to competition between the classical and the quantum contributions to the junction conductance. The classical current, described in terms of the eigenstate populations, and the quantum contribution, that comes from the superposition between the eigenstates, have opposite contributions to the net current. The classical part is always positive (flows along the applied bias) while the quantum contribution is always negative for large couplings. For a serially coupled system, for large couplings (Γ), the classical and the quantum contributions saturate to the same finite value that corresponds to the (quantum) conductivity of a perfect channel. The two contributions therefore tend to cancel each other out completely at large Γ , leading to the net zero current through the junction. On the other hand, for a side-coupled system, the two contributions grow linearly with Γ in opposite directions with the same rate. This results in the net current saturating to a finite value. The coherent contribution in this case is negative for all Γ values.

It is to be noted that while for serially coupled system, the coherent contribution can be positive or negative or even vanish

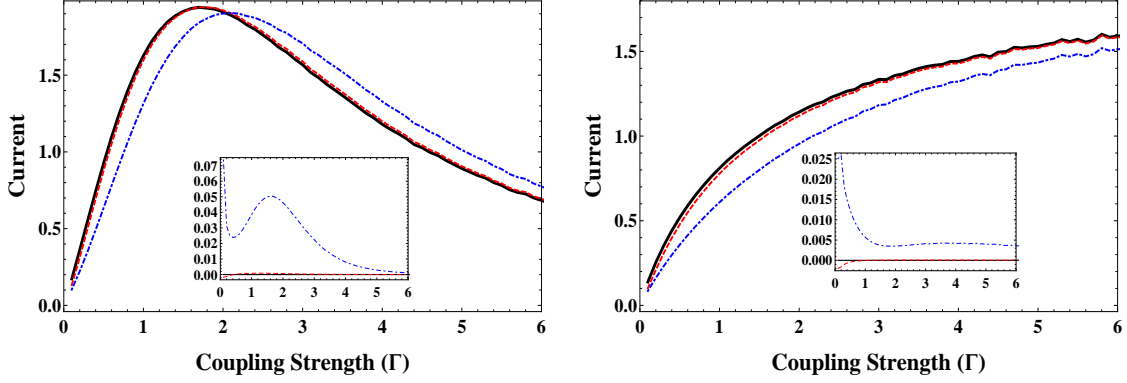


Figure 4: (Color online) Net current as a function of Γ for serially coupled (left) and side coupled (right) double quantum dot system with coulomb interaction treated within HF approximation for $U=0.0$ (continuous), $U=0.1$ (long dashed) and $U=1.0$ (short dashed). Here $t = 1$, $\beta_L = \beta_R = 1000.0$, $\mu_L = \frac{V}{2}$ and $\mu_R = -\frac{V}{2}$ with $V = 2$. All energy scales are in units of t and current is in units of $\frac{e}{\hbar}t$ with $t = 1$. Difference between current calculated within HF and GW approximations for same set of parameters is shown in the inset. The wiggles for larger couplings in the right panel are due to the numerical errors caused by a larger grid spacing chosen for want of computational time.

depending on the system parameters, for a side-coupled system, however, the coherent contribution is always negative and is zero only when the net current vanishes. That is, for a side-coupled system, the coherent channel always conducts in the direction opposite to the applied bias and can not be blocked to maximize the net current, which is possible for a serially coupled system. We found that the qualitative results remain valid even for more realistic junctions with Coulomb interactions.

In order to preserve the left-right symmetry, the partitioning of the current requires a careful choice of the basis. We found that partitioning in the eigenbasis satisfies this criteria, although it does not rule out possibilities of other basis. Within HF approximation, since the single-particle picture is still valid, it is easy to identify the eigenbasis and analyze the current components. Whereas within the GW approximation, the single-particle picture is not valid.

Although not discussed here, we observed that the qualitative behavior of the net current with reservoir couplings as discussed here remains valid even for reservoirs with more general spectral functions (without wide-band approximation). For example, for a Lorentzian bath spectral density, the results for large couplings ($\Gamma > 2t$) remain valid for both model systems. Similarly, for a circular molecular junction, for example symmetric four site cyclic molecular junction, the population and coherences contribute oppositely to the net current for large coupling strengths. This, therefore, seems to be a general trend for currents in molecular junctions. In fact, for a noninteracting electron system, in general, the classical (population) contribution is always positive[48]. The quantum (coherence) contribution, as discussed above, can be positive or negative for small reservoir couplings but become negative for large coupling strengths.

Acknowledgments

H. Y. and U. H. acknowledge the financial support from the Indian Institute of Science, Bangalore, India.

6. Appendix

6.1. Greens function and its equation of motion

Green's functions (in matrix form) are defined on Schwinger-Keldysh contour [56] as,

$$G^c(\tau, \tau') = -\frac{i}{\hbar} \langle [\Theta(\tau, \tau') \Psi(\tau) \Psi^\dagger(\tau') - \Theta(\tau', \tau) \Psi^\dagger(\tau')^T \Psi(\tau)^T] \rangle \quad (21)$$

where τ and τ' are contour times with, $\Psi(\tau) = (c_1(\tau), c_2(\tau))^T$ and $\Theta(\tau, \tau')$ is the Heaviside step function defined on the Schwinger-Keldysh contour. $G^c(\tau, \tau')$ satisfies the following equation of motion

$$\int_c d\tau_1 \left[\left(i\hbar \frac{\partial}{\partial \tau} - H_S \right) \delta^c(\tau, \tau_1) - \Sigma^c(\tau, \tau_1) \right] G^c(\tau_1, \tau') = \delta^c(\tau, \tau') \quad (22)$$

where Σ^c is self-energy due to interaction with the reservoirs and it is given as sum of self energies due to left and right reservoirs i.e., $\Sigma^c(\tau, \tau') = \sum_{\alpha=L,R} \Sigma_\alpha^c(\tau, \tau')$. The self energies due to reservoirs is given by a 2×2 matrix with element (i, j) defined as,

$$[\Sigma_\alpha^c(\tau, \tau')]_{ij} = g_\alpha^{(i)*} g_\alpha^{(j)} \sum_{k,k'} G_{\alpha k, \alpha k'}^0(\tau, \tau'). \quad (23)$$

Here $G_{Lk, Lk'}^0(\tau, \tau')$ and $G_{Rk, Rk'}^0(\tau, \tau')$ are contour ordered Green's functions for the isolated reservoirs. Equation (22) can be projected onto the real times using Langreth rules to obtain the real-time Green's functions [16, 56]. At steady-state all Green's functions become time translation invariant and can be handled easily in the energy domain.

6.2. Self energies due to coulomb interaction

Coulomb interaction adds an extra self-energy to the equation of motion given in 22. Within mean-field approximation,

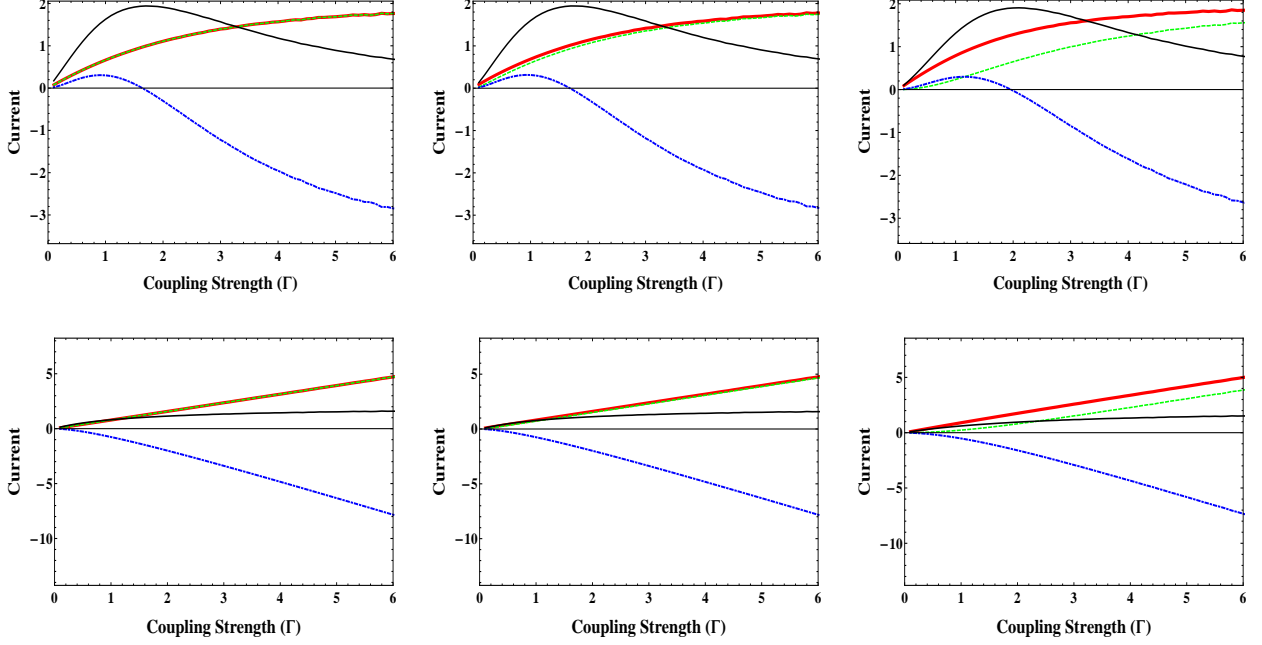


Figure 5: (Color online) Currents carried by bonding (red-thick) state, anti-bonding (green-dashed) state, and coherences between them (blue-dot-dashed) along with the net current (black-thin) for serial coupled case (upper-row) and side coupled case (lower-row) with coulomb interaction between electrons on quantum dots treated within HF approximation, for $U=0.0$ (leftmost column), $U=0.1$ (middle column) and $U=1.0$ (rightmost column). Rest of the parameters are same as in Fig. (4). Note that due to Coulomb interaction, the currents carried by the eigenstates are no longer equal.

the self-energy due to Coulomb interaction is given by,

$$\begin{aligned} \Sigma_{ij}^{MF}(\tau, \tau') &= -i\hbar \sum_{k=1,2} V_{ik} G_{kk}^c(\tau, \tau^+) \delta_{ij} \delta^c(\tau, \tau') \\ &\quad + i\hbar V_{ij} G_{ij}^c(\tau, \tau^+) \delta^c(\tau, \tau'), \end{aligned} \quad (24)$$

where τ^+ is infinitesimally greater than τ , and within GW approximation, the self-energy is obtained as,

$$\begin{aligned} \Sigma_{ij}^{GW}(\tau, \tau') &= -i\hbar \sum_{k=1,2} V_{ik} G_{kk}^c(\tau, \tau^+) \delta_{ij} \delta^c(\tau, \tau') \\ &\quad + i\hbar G_{ij}^c(\tau, \tau') W_{ji}^c(\tau', \tau). \end{aligned} \quad (25)$$

Here W^c is the nonequilibrium screened coulomb interaction which satisfies the following Dyson like equation,

$$\begin{aligned} W_{ij}^c(\tau, \tau') &= V_{ij}(\tau, \tau') + \sum_{k_1=1,2} \sum_{k_2=1,2} \int_c d\tau_1 \int_c d\tau_2 \\ &\quad V_{ik_1}(\tau, \tau_1) P_{k_1 k_2}^c(\tau_1, \tau_2) W_{k_2 j}^c(\tau_2, \tau') \end{aligned} \quad (26)$$

where $V_{ij}(\tau, \tau') = V_{ij} \delta^c(\tau, \tau')$ and $P_{ij}^c(\tau, \tau') = -i\hbar G_{ij}^c(\tau, \tau') G_{ji}^c(\tau', \tau)$ is the nonequilibrium polarization function within GW approximation.

6.3. General result for non-interacting system case

Current carried from right reservoir to left reservoir by the population in the n^{th} system eigenstate coupled to two fermionic reservoirs is given by

$$I_{Lmn} = \int_{-\infty}^{+\infty} d\omega \left[\Sigma_{Lmn}^<(\omega) G_{nm}^>(\omega) - G_{nm}^<(\omega) \Sigma_{Lmn}^>(\omega) \right]. \quad (27)$$

For a noninteracting electron system, this can be expressed in the form

$$I_{Lmn} = \int_{-\infty}^{+\infty} d\omega T_{mn}(\omega) [f_L(\omega) - f_R(\omega)] \quad (28)$$

where the transmission function of the n^{th} state is

$$\begin{aligned} T_{Lmn}(\omega) &= (2\pi)^2 \sum_{k_1, k_2} \delta(\omega - \epsilon_{Lk_1}) \delta(\omega - \epsilon_{Rk_2}) \\ &\quad \times \left| \sum_m g_{Lk_1 n} G_{nm}^r(\omega) g_{Rk_2 m} \right|^2, \end{aligned} \quad (29)$$

which is non-negative for any ω . Hence the population channels (for $\beta_L = \beta_R = \beta$ case) always conduct current in the direction of applied bias. Similarly, the current carried by the coherences between states m and n is given by

$$\begin{aligned} I_{Lmn} &= \int_{-\infty}^{+\infty} d\omega \left[\Sigma_{Lmn}^<(\omega) G_{nm}^>(\omega) - G_{nm}^<(\omega) \Sigma_{Lmn}^>(\omega) \right. \\ &\quad \left. + \Sigma_{Lmn}^<(\omega) G_{mn}^>(\omega) - G_{mn}^<(\omega) \Sigma_{Lmn}^>(\omega) \right]. \end{aligned} \quad (30)$$

This can be simplified to

$$I_{Lmn} = \int_{-\infty}^{+\infty} d\omega T_{mn}(\omega) [f_L(\omega) - f_R(\omega)] \quad (31)$$

where the transmission function,

$$\begin{aligned} T_{Lmn}(\omega) &= (2\pi)^2 \sum_{k_1, k_2} \delta(\omega - \epsilon_{Lk_1}) \delta(\omega - \epsilon_{Rk_2}) \\ &\quad \sum_{p, q} \left[\Gamma_{Lmn}(\omega) G_{mp}^r(\omega) \Gamma_{Rpq}(\omega) G_{qn}^a(\omega) \right. \\ &\quad \left. + \Gamma_{Lmn}(\omega) G_{np}^r(\omega) \Gamma_{Rpq}(\omega) G_{qm}^a(\omega) \right]. \end{aligned} \quad (32)$$

with $\Gamma_{\alpha_m}(\omega) = 2\pi \sum_k g_{\alpha km} \delta_{\alpha kn}^* \delta(\omega - \epsilon_{\alpha k})$, need not always be positive (nevertheless can be shown to be a real quantity).

6.4. Details of numerical solution of equations of motion within HF and GW approximations

Steady state equations of motion for system Greens function (with the appropriate self energy due to coulomb interaction) are Fourier transformed into energy domain, the resulting equations are solved self consistently by discretising the energy domain with grid spacing $\Gamma/500$ and grid range $\approx (-400 * \Gamma + 10 * U, +400 * \Gamma + 10 * U)$. All the energy integrals are numerically evaluated using Simpson's-1/3 rule [57]. Further, convolutions and correlations encountered within GW approximation are calculated using fast Fourier transform [57] as implemented in FFTW3 [58]. Convergence of GW calculations is accelerated using Pulay mixing scheme [59] as implemented in Ref.[52].

References

References

- [1] Massimiliano Esposito, Upendra Harbola, and Shaul Mukamel. Nonequilibrium fluctuations, fluctuation theorems, and counting statistics in quantum systems. *Rev. Mod. Phys.*, 81(4):1665, 2009.
- [2] Yasuhiro Utsumi, DS Golubev, Michael Marthaler, Keiji Saito, Toshimasa Fujisawa, and Gerd Schön. Bidirectional single-electron counting and the fluctuation theorem. *Physical Review B*, 81(12):125331, 2010.
- [3] Arieh Aviram and Mark A Ratner. Molecular rectifiers. *Chemical Physics Letters*, 29(2):277–283, 1974.
- [4] David M Cardamone, Charles A Stafford, and Sumit Mazumdar. Controlling quantum transport through a single molecule. *Nano letters*, 6(11):2422–2426, 2006.
- [5] Marlan O Scully, M Suhail Zubairy, Girish S Agarwal, and Herbert Walther. Extracting work from a single heat bath via vanishing quantum coherence. *Science*, 299(5608):862–864, 2003.
- [6] Himangshu Prabal Goswami and Upendra Harbola. Thermodynamics of quantum heat engines. *Physical Review A*, 88(1):013842, 2013.
- [7] Daniel Loss and David P DiVincenzo. Quantum computation with quantum dots. *Physical Review A*, 57(1):120, 1998.
- [8] Wilfred G Van der Wiel, Silvano De Franceschi, Jeroen M Elzerman, Toshimasa Fujisawa, Seigo Tarucha, and Leo P Kouwenhoven. Electron transport through double quantum dots. *Reviews of Modern Physics*, 75(1):1, 2002.
- [9] NJ Tao. Electron transport in molecular junctions. *Nature nanotechnology*, 1(3):173–181, 2006.
- [10] Dong Xiang, Xiaolong Wang, Chuancheng Jia, Takhee Lee, and Xuefeng Guo. Molecular-scale electronics: from concept to function. *Chem. Rev.*, 116(7):4318–4440, 2016.
- [11] Ioan Bâldea. *Molecular Electronics: An Experimental and Theoretical Approach*. CRC Press, 2016.
- [12] Juan Carlos Cuevas and Elke Scheer. *Molecular electronics: an introduction to theory and experiment*. World Scientific, 2010.
- [13] Gianaurelio Cuniberti, Giorgos Fagas, and Klaus Richter. *Introducing molecular electronics*, volume 680. Springer, 2006.
- [14] Upendra Harbola, Massimiliano Esposito, and Shaul Mukamel. Quantum master equation for electron transport through quantum dots and single molecules. *Physical Review B*, 74(23):235309, 2006.
- [15] Supriyo Datta. *Electronic transport in mesoscopic systems*. Cambridge university press, 1997.
- [16] Hartmut Haug and Antti-Pekka Jauho. *Quantum kinetics in transport and optics of semiconductors*. Springer, 1996.
- [17] Po-Wen Chiu and Siegmur Roth. Carbon nanotube nanocontact in t-junction structures. *Applied Physics Letters*, 91(10):102109, 2007.
- [18] Norbert Nemeč, David Tománek, and Gianaurelio Cuniberti. Modeling extended contacts for nanotube and graphene devices. *Physical Review B*, 77(12):125420, 2008.
- [19] TV Shahbazyan and ME Raikh. Two-channel resonant tunneling. *Physical Review B*, 49(24):17123, 1994.
- [20] Timothy A Su, Madhav Neupane, Michael L Steigerwald, Latha Venkataraman, and Colin Nuckolls. Chemical principles of single-molecule electronics. *Nature Reviews Materials*, 1:16002, 2016.
- [21] Jorge M Seminario, Cecilia E De La Cruz, and Pedro A Derosa. A theoretical analysis of metal- molecule contacts. *Journal of the American Chemical Society*, 123(23):5616–5617, 2001.
- [22] Jeremy M Beebe, Vincent B Engelkes, Larry L Miller, and C Daniel Frisbie. Contact resistance in metal- molecule- metal junctions based on aliphatic sams: Effects of surface linker and metal work function. *Journal of the American Chemical Society*, 124(38):11268–11269, 2002.
- [23] Olgun Adak, Richard Korytár, Andrew Y Joe, Ferdinand Evers, and Latha Venkataraman. Impact of electrode density of states on transport through pyridine-linked single molecule junctions. *Nano letters*, 15(6):3716–3722, 2015.
- [24] Chih-Hung Ko, Min-Jie Huang, Ming-Dung Fu, and Chun-hsien Chen. Superior contact for single-molecule conductance: electronic coupling of thiolate and isothiocyanate on pt, pd, and au. *Journal of the American Chemical Society*, 132(2):756–764, 2009.
- [25] Andrey Danilov, Sergey Kubatkin, Sergey Kafanov, Per Hedegård, Nicolai Stühr-Hansen, Kasper Moth-Poulsen, and Thomas Bjørnholm. Electronic transport in single molecule junctions: Control of the molecule-electrode coupling through intramolecular tunneling barriers. *Nano letters*, 8(1):1–5, 2008.
- [26] SA Gurvitz and Ya S Prager. Microscopic derivation of rate equations for quantum transport. *Physical Review B*, 53(23):15932, 1996.
- [27] Kirill A Velizhanin, Haobin Wang, and Michael Thoss. Heat transport through model molecular junctions: A multilayer multiconfiguration time-dependent hartree approach. *Chemical Physics Letters*, 460(1):325–330, 2008.
- [28] Bijay Kumar Agarwalla and Dvira Segal. Energy current and its statistics in the nonequilibrium spin-boson model: Majorana fermion representation. *New Journal of Physics*, 19(4):043030, 2017.
- [29] Alexander J White, Uri Peskin, and Michael Galperin. Coherence in charge and energy transfer in molecular junctions. *Physical Review B*, 88(20):205424, 2013.
- [30] Sriharsha V Aradhya, Jeffrey S Meisner, Markrete Krikorian, Seokhoon Ahn, Radha Parameswaran, Michael L Steigerwald, Colin Nuckolls, and Latha Venkataraman. Dissecting contact mechanics from quantum interference in single-molecule junctions of stilbene derivatives. *Nano letters*, 12(3):1643–1647, 2012.
- [31] Constant M Guédon, Hennie Valkenier, Troels Markussen, Kristian S Thygesen, Jan C Hummelen, and Sense Jan Van Der Molen. Observation of quantum interference in molecular charge transport. *Nature nanotechnology*, 7(5):305–309, 2012.
- [32] Carlos R Arroyo, Riccardo Frisenda, Kasper Moth-Poulsen, Johannes S Seldenthuis, Thomas Bjørnholm, and Herre SJ van der Zant. Quantum interference effects at room temperature in opv-based single-molecule junctions. *Nanoscale research letters*, 8(1):234, 2013.
- [33] H Vazquez, R Skouta, S Schneebeli, M Kamenetska, R Breslow, L Venkataraman, and MS Hybertsen. Probing the conductance superposition law in single-molecule circuits with parallel paths. *Nature Nanotechnology*, 7(10):663–667, 2012.
- [34] CJ Lambert. Basic concepts of quantum interference and electron transport in single-molecule electronics. *Chemical Society Reviews*, 44(4):875–888, 2015.
- [35] Troels Markussen, Robert Stadler, and Kristian S Thygesen. The relation between structure and quantum interference in single molecule junctions. *Nano letters*, 10(10):4260–4265, 2010.
- [36] Gemma C Solomon, David Q Andrews, Thorsten Hansen, Randall H Goldsmith, Michael R Wasielewski, Richard P Van Duyne, and Mark A Ratner. Understanding quantum interference in coherent molecular conduction. *The Journal of chemical physics*, 129(5):054701, 2008.
- [37] Thorsten Hansen, Gemma C Solomon, David Q Andrews, and Mark A Ratner. Interfering pathways in benzene: An analytical treatment. *The Journal of chemical physics*, 131(19):194704, 2009.
- [38] Matthew G Reuter and Thorsten Hansen. Communication: Finding de-

- structive interference features in molecular transport junctions, 2014.
- [39] David Q Andrews, Gemma C Solomon, Randall H Goldsmith, Thorsten Hansen, Michael R Wasielewski, Richard P Van Duyne, and Mark A Ratner. Quantum interference: The structural dependence of electron transmission through model systems and cross-conjugated molecules. *The Journal of Physical Chemistry C*, 112(43):16991–16998, 2008.
- [40] Feng Chen, Yi Gao, and Michael Galperin. Molecular heat engines: Quantum coherence effects. *Entropy*, 19(9):472, 2017.
- [41] Daijiro Nozaki, Stas M Avdoshenko, Håldun Sevincli, and Gianaurelio Cuniberti. Quantum interference in thermoelectric molecular junctions: A toy model perspective. *Journal of Applied Physics*, 116(7):074308, 2014.
- [42] Colin J Lambert, Hatef Sadeghi, and Qusiy H Al-Galiby. Quantum-interference-enhanced thermoelectricity in single molecules and molecular films. *Comptes Rendus Physique*, 17(10):1084–1095, 2016.
- [43] Roi Baer and Daniel Neuhauser. Phase coherent electronics: a molecular switch based on quantum interference. *Journal of the American Chemical Society*, 124(16):4200–4201, 2002.
- [44] R Härtle, M Butzin, O Rubio-Pons, and M Thoss. Quantum interference and decoherence in single-molecule junctions: How vibrations induce electrical current. *Physical review letters*, 107(4):046802, 2011.
- [45] Stefan Ballmann, Rainer Härtle, Pedro B Coto, Mark Elbing, Marcel Mayor, Martin R Bryce, Michael Thoss, and Heiko B Weber. Experimental evidence for quantum interference and vibrationally induced decoherence in single-molecule junctions. *Physical review letters*, 109(5):056801, 2012.
- [46] Troels Markussen and Kristian S Thygesen. Temperature effects on quantum interference in molecular junctions. *Physical Review B*, 89(8):085420, 2014.
- [47] Yigal Meir and Ned S Wingreen. Landauer formula for the current through an interacting electron region. *Physical review letters*, 68(16):2512, 1992.
- [48] See appendix for more detail.
- [49] Hari Kumar Yadalam and Upendra Harbola. Controlling local currents in molecular junctions. *Physical Review B*, 94(11):115424, 2016.
- [50] Lars Hedin. New method for calculating the one-particle green’s function with application to the electron-gas problem. *Physical Review*, 139(3A):A796, 1965.
- [51] Upendra Harbola and Shaul Mukamel. Nonequilibrium superoperator gw equations. *The Journal of chemical physics*, 124(4):044106, 2006.
- [52] Kristian S Thygesen and Angel Rubio. Conserving g w scheme for nonequilibrium quantum transport in molecular contacts. *Physical Review B*, 77(11):115333, 2008.
- [53] Catalin D Spataru, Mark S Hybertsen, Steven G Louie, and Andrew J Millis. Gw approach to anderson model out of equilibrium: Coulomb blockade and false hysteresis in the i- v characteristics. *Physical Review B*, 79(15):155110, 2009.
- [54] Gianluca Stefanucci and Robert Van Leeuwen. *Nonequilibrium many-body theory of quantum systems: a modern introduction*. Cambridge University Press, 2013.
- [55] F Tandetzky, JK Dewhurst, S Sharma, and EKV Gross. Multiplicity of solutions to g w-type approximations. *Physical Review B*, 92(11):115125, 2015.
- [56] Jørgen Rammer. *Quantum field theory of non-equilibrium states*. Cambridge University Press, 2007.
- [57] William H Press, Saul A Teukolsky, William T Vetterling, and Brian P Flannery. Numerical recipes in c. 1992. *Cambridge: Cambridge University*, 1994.
- [58] Matteo Frigo and Steven G Johnson. The design and implementation of fftw3. *Proceedings of the IEEE*, 93(2):216–231, 2005.
- [59] Péter Pulay. Convergence acceleration of iterative sequences. the case of scf iteration. *Chemical Physics Letters*, 73(2):393–398, 1980.